American Mineralogist, Volume 63, pages 230–238, 1978

Growth-induced radiation-developed pleochroic anisotropy in smoky quartz

KURT NASSAU AND BETTY E. PRESCOTT

Bell Laboratories
Murray Hill, New Jersey 07974

Abstract

The "anomalous pleochroism" of Tsinober is observed in all irradiated synthetic quartz grown on minor rhombohedron seeds. This phenomenon was reexamined, using the absorption dichroism of the ordinary ray in basal sections for detailed study. The anisotropy originates in non-random occupancy by Al of the three equivalent Si sites and can be explained on the basis of a difference in the occupancy selectivity on the two sides of the seed plate. Redistribution of the impurity centers takes place on heating above 490°C. The A_3 smoky absorption (the hextet Al substitutional hole color center) showed different orientations of the absorption maxima on opposite sides of the seed, with dichroic ratios of 1.22 and 1.15, when viewed in polarized light while rotating about the *c* axis. The other absorptions had the same orientations on the two sides of the seed, but their orientations were different from each other. The A_1 absorption showed a dichroic ratio as high as 4.1 and a shape consistent with light interacting with an oscillator lying approximately in the basal plane.

Introduction

Tsinober (1962) and Tsinober *et al.* (1967) have described an "anomalous pleochroism" in smoky (*i.e.*, irradiated) synthetic quartz grown on seed plates cut parallel to the face (10.1) (the minor rhombohedron). The smoky quartz on opposite sides of the seed plate showed different absorption spectra and differing EPR (electron paramagnetic resonance) spectra. The phenomenon was interpreted by these investigators on the basis of non-random Si–Al occupancy of sites related by the three-fold axis and differing non-randomness on the two sides of the seed plate. A common impurity in quartz is Al^{3+} substituting for Si^{4+}, with an alkali ion or proton providing charge compensation. Irradiation ejects an electron from an oxygen adjacent to the Al, resulting in "smoky" quartz. This now shows the well-known hextet hyperfine structure EPR spectrum, which has been correlated with the optical A_3 absorption at 2.9eV (Nassau and Prescott, 1975; 1977).

In a study of amethyst, Hassan and Cohen (1974) observed biaxiality and anomalous dichroism, and related this to the non-random substitution of Fe^{3+} in the equivalent Si sites observed in EPR by Barry and Moore (1964) and Barry *et al.* (1965). Heating was found to remove most of the anomalies in both the smoky quartz and amethyst studies, pointing to a homogenization process. There has been disagreement about the impurity redistribution concept between Lehmann (1975) and Cohen (1975). Differing non-randomness within the same crystal does not appear to have been reported in amethyst.

The phenomenon in smoky quartz was independently discovered in 1970 by R. L. Barns (Bell Laboratories) who brought it to our attention. In view of our interest in the nature of smoky quartz (Nassau and Prescott, 1975; 1977), we have also examined the pleochroic phenomenon. The designations "anomalous pleochroism" and "twinning" (applied previously by Tsinober, 1962) are not satisfactory. Descriptive designations are "differing non-uniaxial pleochroism produced by irradiation, reflecting a growth-induced anisotropy in hydrothermal quartz," or the title designation.

Experimental

The synthetic quartz bars studied had been grown in steel vessels under hydrothermal conditions (82% fill of 1.0M NaOH + 0.025M Li_2CO_3, growth temperature 350°C with ΔT 50°C, and growth rate about 0.9 mm/day), at the Western Electric Company (Barns *et al.*, 1976). Crystals grown in silver vessels showed the same effect. Most work was performed on crystals grown on minor rhombohedral seeds, type *z* (10.1), as shown in the center of Figure 1. Slices were

0003–004X/78/0304–0230$02.00

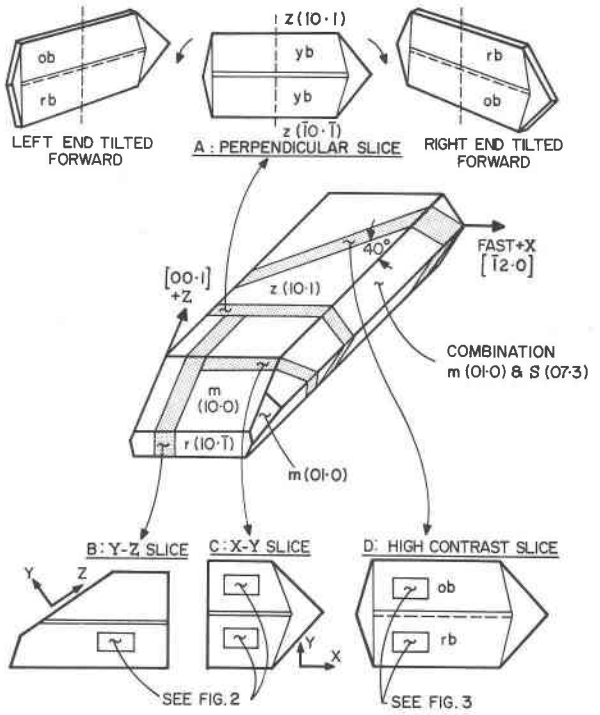

Fig. 1. Sketch of synthetic quartz crystal #LC 3237-15 and slices studied. Rectangles indicate areas where absorption spectra were taken; ob is olive brown, yb is yellowish brown, and rb is reddish brown.

cut from crystal #LC 3237-15 as indicated, and the appearance after room-temperature irradiation with 15 megarads of Co-60 gamma rays is indicated: Figure 1A, a slice perpendicular to the z face and parallel to the X axis; Figures 1B and C, Y–Z slice and X–Y (basal section); Figure 1D, a high contrast slice, as discussed below. Growth on the major rhombohedron and on the basal surface was also studied but did not appear to show any anomalous behavior.

Polarized optical spectra (σ with E perpendicular to c, π with E parallel to c) were taken at room temperature on a Cary 14R spectrophotometer in the range 1.0 to 5.7eV (1.2 to 0.22μm). The specific absorbance, $\alpha = (1/t)\log_{10}(I_0/I)$ where t is the sample thickness in cm, was calculated without reflectance correction. Gaussian curve fitting was performed as previously described (Nassau and Prescott, 1975).

Emission spectrographic analyses were made on samples cut symmetrically from the upper and lower parts of crystal #LC 3237-15.

Results and discussion

Irradiation of over 80 crystals of synthetic quartz grown on the minor rhombohedron gave results essentially identical to those for crystal #LC 3237-15. After irradiation, a brown coloration was seen in each case on both sides of the seed, a medium-yellowish brown approximately #77 (Kelly and Judd, 1965) as seen in a 3 mm slice. On tilting the slice about an axis perpendicular to the minor rhombohedral growth face, one side acquired a greenish tint (medium olive brown #95) and the other side a reddish tint (medium reddish brown, #43). Rotation in the opposite direction reversed these colors. This behavior is illustrated in Figure 1A.

The dichroic spectra of Figure 2 indicate relatively small differences in the absorptions with the direction of polarization in the Y–Z and X–Y slices. The σ curve of the Y–Z slice is similar to curves 1, 5, and 6 given by Tsinober *et al.* (1967), where some germanium had been present during growth.

The angled slice shown in Figure 1D was cut at an orientation estimated to be near the direction for maximum color difference between the upper and lower parts of the crystal, giving a strong color contrast between the two halves of the slice. The polarized spectra of both sides of this slice are shown, with their Gaussian components, in Figure 3. It was not possible to obtain even an approximate fit by varying

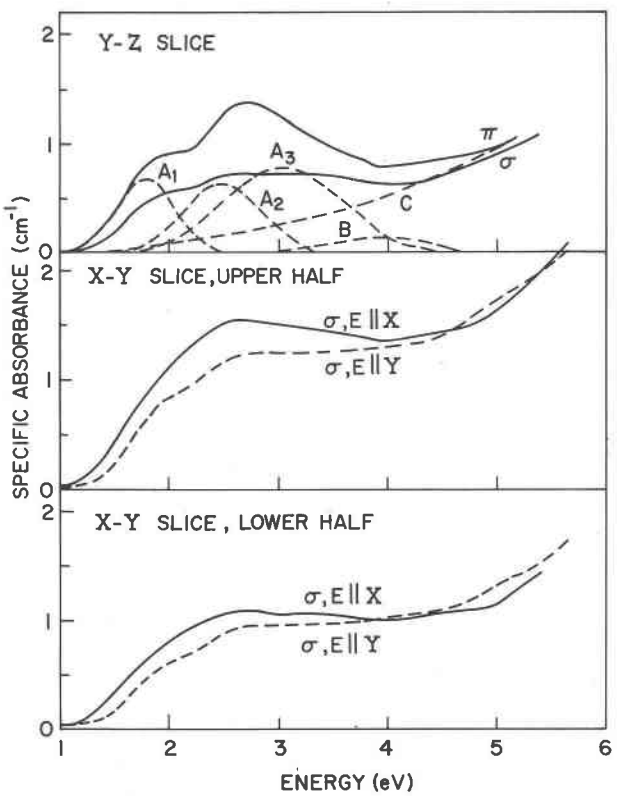

Fig. 2. Polarized absorption spectra of the Y–Z and X–Y slices of Fig. 1B and C.

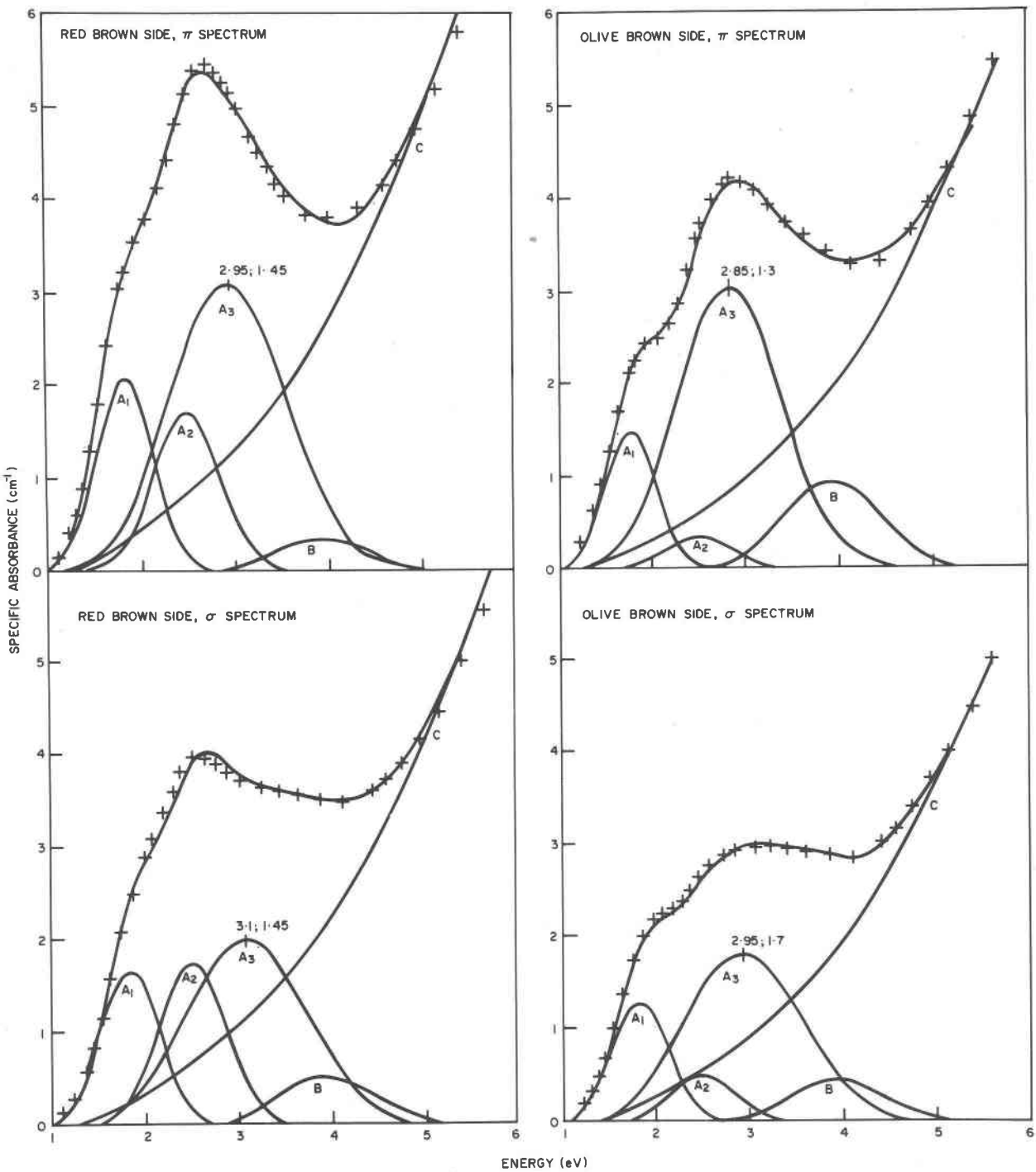

Fig. 3. Polarized absorption spectra of the high contrast slice of Fig. 1D; here σ indicates E perpendicular, and π indicates E parallel, to the projection of the z axis into the plane of the slice.

only the intensity of the A_1, A_2, A_3, B, and C bands, as had been successfully done with all previous samples tested. However, the satisfactory fit of Figure 3 was obtained by slightly shifting the peak position and increasing the half-width of only A_3: 2.85 to 3.1eV instead of the usual 2.9eV for the peak position and 1.3 to 1.7eV instead of the usual 1.5eV for the half-width. These changes in the A_3 band were not

completely unexpected, since this is the band caused by the hextet aluminum-hole center (Nassau and Prescott, 1975) with different non-equivalent occupancy of Si sites on opposite sides of the seed according to Tsinober *et al.* (1967).

An additional effect noted in Figure 3 is that the A_1 and A_2 bands are about equal in intensity on the red-brown side, but A_1 is much stronger than A_2 on the olive-brown side, in both the σ and π spectra. This would indicate that the A_2 band is also connected with the growth-induced anistropy, although the possibility of this being an artifact cannot be ruled out at present.

It was necessary to consider the possiblity of twinning, as initially proposed by Tsinober (1962). Indeed, there is a clearly identifiable boundary surface on one side of the seed in each of our crystals. In the crystal shown in Figure 1 the seed had apparently been cut from the "lower" part of a similar crystal, so that the contact between the two regions here is on the "upper" side of the seed plate, Figure 1D. This phenomenon is not due to Dauphiné-law electrical twinning (checked by etching experiments by E. D. Kolb, Bell Labs), not due to Brazil-law optical twinning (checked by polariscope examination in the unirradiated state by R. L. Barns, Bell Labs), nor can any inclined-axis twin law be involved. It may be noted that brief examination of a Brazil quartz crystal slice irradiated in 1940 by C. Frondel (unpublished observation) showed a similar appearance, however, in this case, across a twin boundary.

For this phenomenon to be a "color center twinning" in the strict sense, at least three conditions would be necessary: (a) the "hole" would need to be able to move freely among the four oxygens surrounding the aluminum, as has been observed (Schnadt and Raüber, 1971); (b) the hole centers on the three otherwise equivalent silicon sites would have to be related to one another by the reflections, translations, and/or rotations involved in the twinning relationship; and (c) the occupancy ratios on the two sides of the seed would have to be the same for the three equivalent sites as related by the twin law. In the specimen examined by Tsinober *et al.* (1967), the EPR intensity ratio of three non-equivalent aluminum-hole centers was 8:1.5:1, changing to 3:1.2:1 after heating to approx. 650°C. It seems most unlikely that conditions (b) and (c) for a valid twinning relationship could ever be met and, accordingly, the designation "twinning" is not appropriate.

External growth factors can be eliminated as causing this phenomenon. Flow in the hydrothermal vessels is turbulent and is controlled by a baffle; all crystals, whether positioned high or low, centrally or radially, showed the same effect. Seed plates are supported vertically, so that gravity can have no effect.

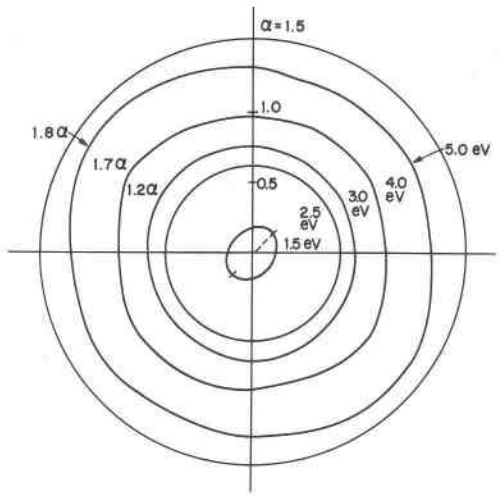

Fig. 4. Polarized rotation absorption curves in the basal plane of a natural Brazil quartz specimen #63076. Absorption coefficient α is plotted radially from the center; the outermost ring is a reference circle. The α of the outer three curves is multiplied by the factors shown so as to separate the curves for clarity. The dotted line is the direction of maximum absorption. Arbitrary orientation.

The spectrographic analysis of crystal #LC 3237-15, Figure 1, showed Fe to be 0.001% in the upper (*u*) part and 0.003% in the lower (*l*) part; Al = 0.0005% *u*, 0.001% *l*. Semi-quantitative results of both parts showed Mg = 0.000*X*%; B = 0.000*X*%; and Cu = 0.000*X* (low) %. All the other elements, detectable by spectrographic analysis (including Ge, which had not been added) were not detected.

Quartz with space group $P3_221$ (LePage and Donnay, 1976) has the three equivalent Si positions $u,0,0$; $0,u,1/3$; and $-u,-u,2/3$. Unequal occupancy of these sites by Al thus automatically leads to a lowering of symmetry to either monoclinic (point group 2) or triclinic (point group 1). A lower space-group symmetry than that of quartz is expected, since the aluminum hole center involved in the A_3 center of smoky quartz has only two-fold site symmetry along the three-fold quartz symmetry direction (Schnadt and Schneider, 1970). This automatically leads to one of the biaxial systems and pleochroism (trichroism).

Considerable insight can be gained from absorption studies of basal sections by rotation of the plane of polarized light about the *c* axis, *i.e.*, examining only the ordinary ray. Figures 4 and 5 are such ordinary-ray rotational plots, taken at 15 or 30° intervals in the basal plane, with the distance from the center

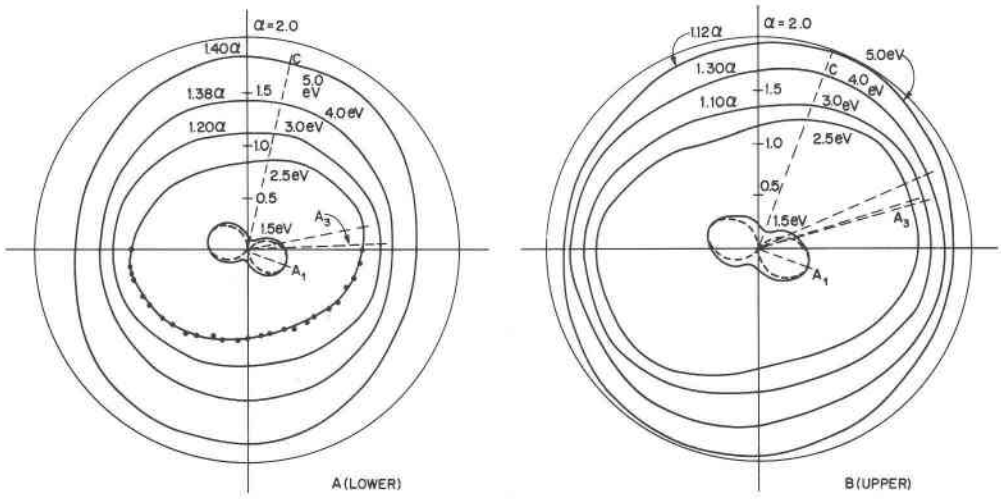

Fig. 5. Polarized rotation absorption curves in the basal plane for the lower and upper halves of the $X-Y$ slice of Fig. 1C; horizontal axis is the projection of the X axis of seed; other details as in Fig. 4.

being proportional to the absorption coefficients. The orientation of the maximum absorption α_{max} was determined by overlaying each plot with a duplicate but inverted plot and rotating to obtain the best fit between each curve and its mirror image. In each case the minimum absorption α_{min} appeared to be at 90° to α_{max}. The error limits given in Table 1 are estimates of the precision of this procedure. The basal plane dichroic ratio is calculated as $\alpha_{max}/\alpha_{min}$, as was done by Hassan and Cohen (1974).

In a truly uniaxial crystal there will be no variation in the optical properties on such rotation, as is found in the examination of a slice of natural smoky Brazilian quartz (#63076) shown in Figure 4. With the exception of a small anomaly in the A_1 band as shown by the 1.5eV curve which has a dichroic ratio of 1.3, all the wavelengths show essentially circular curves having dichroic ratios of 1.03 to 1.08, which are within the experimental error of unity expected for uniaxiality.

Quite different results were obtained for the two halves of the $X-Y$ slice of Figure 1C, as shown in Figures 5A and B. The experimental points are shown for only one half of one curve in Figure 5A; the fit for the other curves was equally satisfactory. Table 1 shows dichroic ratios as high as 4.1 (much

Table 1. Anisotropy of the ordinary ray*

Energy	Major bands	Orientation of α_{max}(°)		Value of α_{max}(cm^{-1})		Dichroic ratio**	
(eV)	present	ℓ	u	ℓ	u	ℓ	u
1.5	A_1	-20±3	-20±5	0.4	0.50	4.1	3.0
2.5	A_3, A_2	+12±5	+17±3	1.11	1.53	1.35	1.37
2.5†	A_2†	+15±8	+19±5	0.21-1.11	0.27-1.53	1.35-4.9	1.37-3.6
3.0	A_3	+3±5	+16±3	1.08	1.50	1.15	1.22
4.0	C, B, A_3	††	+24±8	1.00	1.36	<1.03	1.08
5.0	C	+77±8	+69±8	1.34	1.77	1.12	1.08

*From X-Y slice of Figs. 1C, 5A, and 5B (ℓ for lower, u for upper).

**Dichroic ratio in the basal plane = $\alpha_{max}/\alpha_{min}$; estimated accuracy ±5%.

†Based on $\alpha_{2.5eV}-x\alpha_{3.0eV}$ where $0 < x < 0.90$ for ℓ and $0 < x < 0.85$; larger values for x produce negative α's.

††Dichroic ratio is too small for an approximate determination.

higher than the 1.92 observed by Hassan and Cohen, 1974, in amethyst) and considerable variation in the orientation of the maximum absorption α_{max}.

In the absence of irradiation, the presence of unequal occupancy of the three equivalent Si sites by typically 0.01% Al and the consequent lowering of the symmetry could not be revealed by any known examination technique; the refractive-index ellipsoid would be expected to remain indistinguishable from being uniaxial. This still remains approximately so after irradiation, since significant biaxiality was not observed; but now the absorption indicatrix (the absorption coefficient as a function of vibration direction) becomes a sensitive test for symmetry.

The curves of Figures 4 and 5, in fact, show the cross-sections of the absorption indicatrix in the plane perpendicular to the *c* axis (basal section) and clearly indicate the variability of these figures with wavelength, *i.e.*, in the different absorptions A_1, A_2, A_3, B, and C. This leads directly to the variation of color on tilting of the slice of Figure 1A.

Inspection of the Gaussian composition of Figures 2 and 3 shows that the 1.5eV absorption is predominantly due to A_1; A_3 dominates at 3.0eV; and C at 5.0eV. The B absorption at 4.0 is relatively buried by the C and A_3 contributions, and little can be said about its anisotropy. At 2.5eV, variable amounts of the A_2 and A_3 absorptions are present. By subtracting varying amounts of the 3.0eV absorption from the 2.5eV absorption, it is possible to obtain an estimate of the A_2 band characteristics. This is shown in Figure 6 from the data of Figure 5A; similar results are obtained from the Figure 5B data. Although the dichroic ratio for A_2 depends strongly on the value of x in $\alpha_{2.5eV}-x\alpha_{3.0eV}$, the orientation of α_{max} of A_2 remains in a very narrow region, as also shown in Table 1.

Of the various absorption features in smoky quartz (Nassau and Prescott, 1975), only the A_3 band has been definitely identified, deriving from the substitution of Al for a Si, with an alkali or H^+ providing charge compensation. From Table 1 the basal plane dichroic ratios for A_3 are relatively small (1.15 and 1.22), confirming that these are several overlapping absorptions or that the orientation of the maximum absorption lies at a large angle to the basal plane (*cf.* high contrast slice in Fig. 1). The relatively large shift of 13° ± 6 in orientation between the absorption maxima of the A_3 band (3.0eV) on the two sides of the seed plate indicates that the occupational discrepancy is significantly different for the two sides. All the other absorption bands of Figure 5 and Table 1 show no significant differences in orientation between the two sides. The A_1 and A_2 absorptions show quite large dichroic aspect ratios in the basal plane, ranging up to 4.1. The curves for the A_1 absorption bands at 1.5eV in Figures 5A and B closely approximate the dashed curves $\alpha = \alpha_{max} \cdot \cos^2\theta$, as would be expected for the interaction of the electric field of a light wave with a single oscillating dipole moment at angle θ to each other (Kauzmann, 1957, p. 576). Clearly, the origin of the A_1 absorption (presently unknown) must lie predominantly in a single color center having an oscillating electric moment lying approximately in the basal plane. Multiple centers (even if crystallographically equivalent) or single centers not in the basal plane would show aspect ratios close to unity, as is observed for the other absorptions of Table 1.

The maximum absorptions of the C bands occur approximately 90° from those of the A_1 bands (97° ± 8 and 89° ± 9), but in both lower and upper slices the dichroic ratios of C are not far enough from circularity for this result to be unequivocal. Corresponding values for A_2 and C are 62° ± 11 and 50° ± 9 and for A_1 and A_2 are 35° ± 8 and 39° ± 7 (Fig. 5, Table 1).

Tsinober (1967) had noted that the EPR intensity ratio 8:1.5:1 was changed to 3:1.2:1 after heating for several hours at about 650°C. This was viewed as a migration of Al impurities among tetrahedra, leading to a leveling out of the non-random occupancy. This use of such a high annealing temperature, however, raises the possibility that the α to β transition in quartz may have been essential to this migration.

A part of the lower section of the slice used for Figure 5B and Table 1 was heated for 4 hours at 650°C, and another part for 21 days at 490°C, well below the α–β transition temperature of 573°C. In both cases, the resulting absorption curves after reirradiation resembled those of Figure 4, with dichroic ratios of about 1.6 at 1.5eV and 1.03 to 1.14 at the other wavelengths, equal to or less than the equivalent values in Table 1. Accordingly, the redistribution of the color center (involving the movement of Al ions or, more likely, of charge compensators) occurs at temperatures as low as 490°C, and the α–β quartz transition is not involved. On the question of motion of metal ions at such low temperatures, the amethyst discussion between Lehmann (1975) and Cohen (1975) is relevant.

A proposed site selectivity mechanism

Site-selection impurity distributions in laboratory grown crystals have been reported for Gd in Al_2O_3 (Geschwind and Remeika, 1961) and in the rare-earth iron garnets. The latter are made magnetically

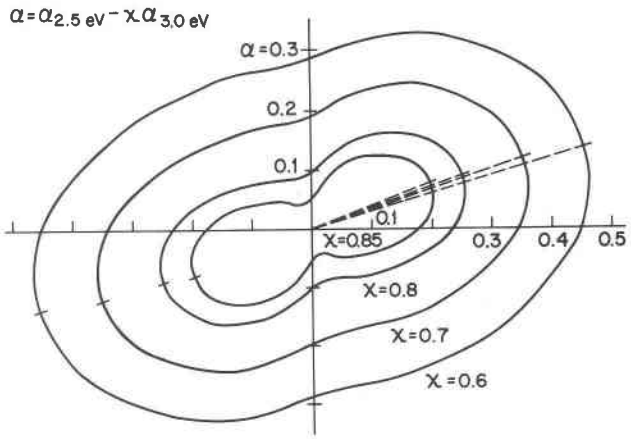

Fig. 6. Inferred polarized rotation absorption curves for absorption band A_2 based on Fig. 5A using $\alpha = \alpha_{2.5eV} - x\alpha_{3.0eV}$ with $0.6 < x < 0.85$; orientation same as Fig. 5.

anisotropic by preferential occupancy of particular sites, and this has been interpreted on the basis of pair ordering and size effects (Callen, 1971; Rosencwaig *et al.*, 1971; Wolfe *et al.*, 1971). Recently it has been recognized that both size and charge effects are significant in these garnets, and that it is the configuration of selected sites with respect to the growth interface that appears to control the site selectivity (Wolfe *et al.*, 1976; R. Wolfe, Bell Labs, in preparation).

A similar approach can be used to postulate the following mechanism for the growth-related anisotropy in quartz. Examination of a three-dimensional model of the quartz structure shows prominent tightly-packed layers of tetrahedra with approximately planar oxygen layers parallel to the minor rhombohedral face (10.1). Such layers of tightly packed polyhedra usually delineate successive positions of the growth interface and produce crystal faces during crystal growth (Jackson, 1967).

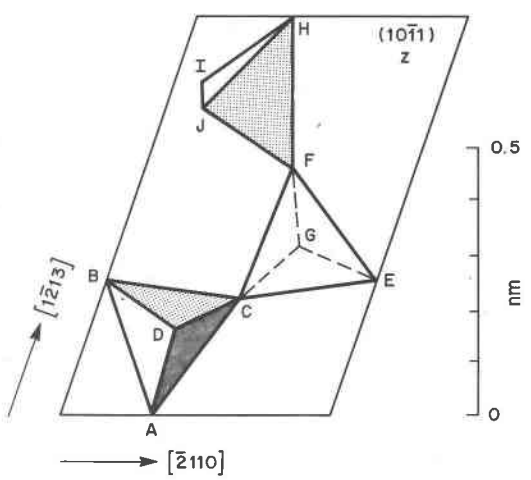

Fig. 7. Projection of the equivalent SiO_4 octahedra in quartz onto the minor rhombohedral surface (10.1).

A projection of the three equivalent SiO_4 tetrahedra onto the (10.1) plane is shown in Figure 7. Two of these tetrahedra have faces in the plane of the drawing, *ABC* and *CEF*; corner *D* lies above and corner *G* lies below this plane. The *FHIJ* tetrahedron lies with the *IJ* edge bisected by the plane of the drawing. This last tetrahedron is symmetrically disposed with respect to the plane and therefore cannot contribute to any growth-related anisotropy of the type being proposed.

When the tetrahedra *ABCD* or *CEFG* are being constructed by the addition of AlO_x units from the solution (or, more precisely, from the oxygenated/hydrated aluminum ion complexes present in solution), possibly also accompanied by a charge compensating ion such as H^+, it is clear that there will be a difference in the energy of substitution for these two sites. For growth upward out of the plane of Figure 7, occupation of *CEFG* corresponds to filling up a tetrahedral "hole" in an almost completed layer, while occupation of *ABCD* corresponds to starting a new layer. For growth downward into the plane of Figure 7, these relationships are reversed.

Thus, if aluminum tends to concentrate (with respect to the average aluminum concentration in the quartz crystal) preferentially at *ABCD* during upward growth, it will correspondingly concentrate at *CEFG* during downward growth, the result being a site selectivity associated with the direction of growth. Alternatively, concentration at *CEFG* during upward and *ABCD* during downward growth still produces the same result. The occupancy ratio of 8:1.5:1 of Tsinober *et al.* (1967) confirms that a single site arrangement is selective.

Examination of other projections shows that for the dominant growth surfaces observed in synthetic quartz (prism and rhombohedral faces, basal plane surface), only the minor rhombehedral face has a clear-cut configuration leading to a growth anisotropy, *i.e.*, only these growth faces show a strong preferential presentation of just one of the sites which are equivalent by the trigonal symmetry. For major rhombohedral growth there is a similar, but much less pronounced up–down relationship; for prism growth the same crystallographically-equivalent sites present themselves in an identical manner in opposite growth directions, and for basal growth successive positions of the growth interface present the three

equivalent sites one at a time; none of these growth directions could therefore lead to a strong growth anisotropy.

In laboratory hydrothermal growth of quartz, rapid growth occurs only on the major and minor rhombohedral faces and on the basal surface (*e.g.*, in 5°*X* crystals, Laudise and Sullivan, 1959). Of these three growth directions, only the minor rhombohedral growth shows the growth anisotropy. We have observed similar color changes in growth in the fast *X* direction, *i.e.*, under the stepped *m*(01.0) and *S*(07.3) development (see Fig. 1). In the opposite slow *X* direction, which shows a much more complex stepped development, there are small regions giving the same colors but on opposite tilting, *i.e.*, olive-brown when the bulk of the slice as well as the fast *X* regions are being seen as reddish-brown, and vice versa. Growth in these directions is very slow and only very small specimens are available; therefore, we have not studied these aspects. Growth on the prism faces is too slow (Kleschev *et al.*, 1976) for its nature to be determined.

Other mechanisms for producing anisotropy may be possible, but it should be noted that the polar axes are almost certainly not involved: positive and negative polar axes alternate every 60° in the basal plane of the quartz structure in the six $\langle 11\bar{2}0 \rangle$ directions; the combination of these axes results in zero polarity perpendicular to the rhombohedral faces.

Visual examination of a sectored amethyst crystal slice from India showed color variations on tilting within the sectors, which may be indicative of a similar pleochroic growth anisotropy due to site selectivity, here involving Fe; this has not been further investigated.

Summary

It is possible to attribute the growth-induced radiation-developed pleochroic anisotropy in smoky synthetic quartz (the "anomalous pleochroism" of Tsinober, 1967) to the site-selective distribution of Al ions, possibly accompanied by charge-compensating ions, during growth on the minor rhombohedral faces.

There was only one significant difference between material growing on opposite minor rhombohedral faces, as determined by optical absorption studies: the A_3 smoky absorption showed different orientations of the absorption maxima of the ordinary ray in basal-plane sections. Heating experiments showed that the α to β phase transition is not involved in the thermal redistribution of light-absorbing centers.

The A_1 absorption at 1.5eV shows a behavior consistent with that arising from a color center consisting of an oscillating dipole moment of fixed orientation lying approximately in the basal plane. The absorptions A_2, A_3, and C originate either in several overlapping orientations or in a single orientation which lies at a sufficient angle from the basal plane to hide its nature. Only a full three-dimensional determination of the absorption indicatrix at different wavelengths could clarify this point.

Acknowledgments

Helpful discussions with C. Frondel of Harvard, H. Winchell of Yale, and particularly with R. L. Barns and D. L. Wood of the Bell Laboratories are gratefully acknowledged.

References

Barns, R. L., E. D. Kolb and R. A. Laudise (1976) Production and perfection of "*z*-face" quartz. *J. Crystal Growth, 34*, 189–197.

Barry, T. I. and W. J. Moore (1964) Amethyst: optical properties and paramagnetic resonance. *Science, 144*, 289–290.

———, P. McNamara and W. J. Moore (1965) Paramagnetic resonance and optical properties of amethyst. *J. Chem. Phys., 42*, 2599–2606.

Callen, H. (1971) Growth induced anisotropy by preferential site ordering in garnet crystals. *Appl. Phys. Lett., 18*, 311–313.

Cohen, A. J. (1975) On the color centers of iron in amethyst and synthetic quartz: a reply. *Am. Mineral., 60*, 338–339.

Geschwind, S. and J. P. Remeika (1961) Paramagnetic resonance of Gd^{3+} in Al_2O_3. *Phys. Rev., 122*, 757–761.

Hassan, F. and A. J. Cohen (1974) Biaxial color centers in amethyst quartz. *Am. Mineral., 59*, 709–718.

Jackson, K. A. (1967) A Review of the Fundamental Aspects of Crystal Growth. In H. S. Peiser, Ed., *Crystal Growth*, p. 17–24. Pergamon Press, New York.

Kauzmann, W. (1957) *Quantum Chemistry*. Academic Press, N. Y.

Kelly, K. L. and D. B. Judd (1965) *The ISCC-NBS Method of Designating Color and a Dictionary of Color Names* (including the supplement: ICSS-NBS Color Name Charts Illustrated with Centroid Colors). Circular 533, 2nd Ed., Natl. Bur. Stand., U. S. Govt. Printing Office, Washington, D. C.

Kleshchev, G. V., A. N. Bryzgalov, L. N. Chernyi, A. F. Kuznetsov and P. I. Nikitchev (1976) Some trends in shape production for artificial quartz crystals. In N. N. Sheftal, Ed., *Growth of Crystals*, Vol. 12, p. 147–153. Consultants Bureau, New York.

Laudise, R. A. and R. A. Sullivan (1959) Pilot plant production—synthetic quartz. *Chem. Eng. Prog., 55*, 55–59.

LePage, Y. and G. Donnay (1976) Refinement of the crystal structure of low quartz. *Acta Crystallogr., B32*, 2456–2459.

Lehman, G. (1975) On the color centers in amethyst and synthetic quartz: a discussion. *Am. Mineral., 60*, 335–337.

Nassau, K. and B. E. Prescott (1975) A reinterpretation of smoky quartz. *Phys. Status Solidi, A29*, 659–663.

——— and ——— (1977) Smoky, blue, greenish-yellow, and other irradiation related colors in quartz. *Mineral. Mag., 41*, 301–312.

Rosencwaig, A., W. J. Tabor, and R. D. Pierce (1971) Pair-preference and site-preference models for rare-earth iron garnets exhibiting noncubic magnetic anisotropies. *Phys. Rev. Lett., 26*, 779–783.

Schnadt, R. and A. Raüber (1971) Motional effects in the trapped-hole center in smoky quartz. *Solid State Comm., 9*, 159–161.

——— and J. Schneider (1970) The electronic structure of the trapped-hole center in smoky quartz. *Phys. kondens. Mater., 11*, 19–42.

Tsinober, L. I. (1962) A feature of the pleochroism of colored synthetic quartz. *Sov. Phys.-Crystallogr., 7*, 113–114.

———, M. I. Samoilovich, L. A. Gordienko and L. G. Chentsova (1967) Anomalous pleochroism in synthetic smoky quartz crystals. *Sov. Phys.-Crystallogr., 12*, 53–56.

Wolfe, R., M. D. Sturge, F. R. Merritt and L. G. VanUitert (1971) Facet-related site selectivity for rare-earth ions in yttrium aluminum garnets. *Phys. Rev. Lett., 26*, 1570–1573.

———, R. C. LeCraw, S. L. Blank and R. D. Pierce (1976) Growth-induced anisotropy in bubble garnet films containing calcium. *AIP Conference Proceeding #34*, p. 172–174. Joint MMM-Intermag. Conference, Pittsburgh (1976); American Institute of Physics, New York.

Manuscript received, June 20, 1977; accepted for publication, November 3, 1977.